International Journal of Natural and Engineering Sciences
E-ISSN: 2146-0086 17(2): 70-78, 2023
Research Article

Investigation of thermoelectric heat transport adding peltier effect on stabilizing intermediate resistance level for a nanoscale square heater contact electrode phase change memory device

Ibrahim Cinar[1,*]

[1]*Karamanoglu Mehmetbey University, Medical Imaging Techniques, Karaman, Turkey*

*Corresponding author: icinar@kmu.edu.tr

(Received: July 25, 2023 / Accepted: August 25, 2023

Abstract

Phase change memory (PCM) with having high signal to noise ratio, GHz scale write, low power consumption and read rates, scalability, long term reliability are being considered one of the candidates for future data storage technologies. However, without understanding the behavior of thermoelectric heat transport effect with Peltier effect, constructing a 3D finite element modeling is not completed to visualize the complex nature of phase switching dynamics of a phase change material of a PCM device, especially for square like heater electrode causing heterogeneous phase distribution. With this study, I report the investigation of thermoelectric heat transport adding Peltier effect for nanoscale square contact electrode phase change memory device. Therefore, I constructed a 3D finite element modelling by using multiphysics approach to cover electrical, thermal, phase change kinetics, percolation effect and especially thermoelectric effect with Thomson and Peltier effect. With square heater electrode, anisotropic heating profile was obtained for the cases of with thermoelectric heat transport and without thermoelectric heat transport. Normally, square like heater electrode PCM devices has a middle resistance level due to mixture phase of crystalline and amorphous phase. However, in this study, depending on thermoelectric effect, an abrupt switching was observed in without case, although in the thermoelectric heat transport case a stable middle resistance level was obtained. Therefore, this is an evidence of importance of thermoelectric heat transport effect to construct a correct 3D finite element model of a nanoscale square like heater electrode PCM device. This model successfully foresees the necessity of thermoelectric effect to design a PCM device leading to ultra-high density data storage applications..

Keywords: phase change dynamics, thermoelectric heat transport, peltier effect, 3d finite element modelling, middle resistance level

Introduction

Phase change memory (PCM) with having high signal to noise ratio, GHz scale write, low power consumption and read rates, scalability, long term reliability are being considered one of the candidates for future data storage technologies [1-5]. Beside all these their extraordinary properties, having high contrast between 0 and 1 logic states possesses a possibility to create multiple logic levels in a single bit PCM device. As a phase change material, $Ge_2Sb_2Te_5$ (GST) has been widely used in PCM technologies due to their exceptional electrical, thermal and optical properties [2, 6-9]. Especially, one of the reason of selection GST as a based material in PCM device is the large contrast between crystalline and amorphous phase. This makes GST a potential material to fabricate multiple-bit-per-cell device with a mixture phase of crystalline and amorphous phase leading to a stable intermediate state. In literature, there are many methods like, doping materials [10-12], constructing multilayer stack to create an intermediate state [13-14] and so on, however there is also another method to create intermediate state by modification of the site geometry of heater electrode [15]. Although having different kind of methods for intermediate state, to understand switching dynamics of phase change material, 3D simulation is one of the most efficient method to visualize the behavior of the device during switching. However, due to increasing the temperature in the device above 900 – 1000 K, thermoelectric heat transport (THT) effect must be considered [16-19]. THT effect known as Thomson and Peltier effect should be taken into account for finite element modeling [15, 17, 20, 21]. In this study ,the aim is to show the effect of THT, especially with adding Peltier effect in nanoscale square heater electrode PCM device having inhomogeneous phase distribution due to current crowding by site geometry of electrode. For this reason, 3D finite element modeling was constructed to observe heterogonous current

distribution and the effect of THT on switching dynamics of PCM device. Also, THT effect on stabilizing intermediate state is investigated with this simulation to design a multiple data storage media.

Materials and Methods

Device geometry and Boundary Conditions

50 nm thickness phase change active layer ($Ge_2Sb_2Te_5$) is sandwiched between 150 m thick WTi top contact electrode and 30 nm bottom TiN heater metal electrode (see Figure 1). Below the TiN heater electrode there is another 150 nm WTi electrode. Above of WTi top electrode, 250 nm Au layer is used for to take good contact and SiO_2 is used to isolate the device from the environment, especially to isolate heater TiN bottom electrode.

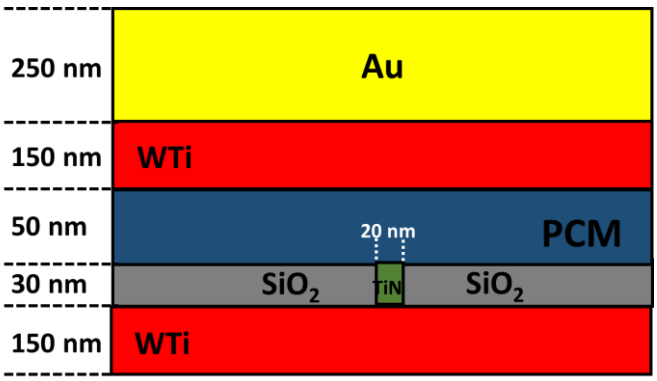

Figure 1. *General phase change memory cell structure: 20 nm square TiN bottom electrode. On top of the WTi top electrode, an Au acts as the contact electrode for device, and SiO_2 is used as isolation.*

For boundary condition for the simulation, both electrical and thermal boundary conditions are set for all side boundaries as the Dirichlet boundary condition ($\Delta y + y = 0$) and for interface surfaces as Neumann boundary condition ($\Delta^2 y + y = 0$). Here Neumann boundary condition refers continues and therefore it is applied for interfaces between PCM- TiN and PCM – WTi. For top and bottom surface, thermal condition is set as 300 K.

Finite Element Model

In a phase change memory cell simulation, electrical and thermal including especially thermoelectric effect and phase change dynamics should be considered to cover the complete behavior of phase change material during phase switching (in this simulation $Ge_2Sb_2Te_5$ (GST) is used as phase change material) . For this reason, I constructed a 3D finite element simulations to see the heater electrode shape effect on material phase change in case of with or without THT (Thomson and Peltier effect), as well as the importance of heater electrode shape in stabilizing the middle resistance level. To oversee the whole dynamics of GST during set operation, simulation was constructed with submodels covering electrical, thermal and kinetics as well as to account for the relation between electrode shape and thermoelectric effects on phase switching from crystalline to amorphous phase. Normally, the complex nature of phase change requires well defined simulation model because of being sensitive for temperature distribution, applied voltage and defect density. Beside all of them, changing the heater shape from circular to square makes the system more complex due to inhomogeneous current distribution causing heterogenetic crystallite change during phase change in material. (For more detail in Cinar 2015) In the simulation, adaptive meshing is used for 2x2x2 nm^3 to obtain more sensitive the results seeing a whole picture of the phase change. Electrical submodel, solving Laplace equation to see potential distribution depending on temperature, phase and electrical conductivity, to solve heat diffusion equation to obtain the joule heating including THT, thermal submodel, and phase change submodel to obtain temperature dependent switching kinetics, were constructed in a multiphysics approach including nonlinear interactions between submodels. [15, 22-25]

Table 1. *Parameters used in simulation; thermal and electrical conductivities, Seebeck coefficient, as well as heat capacity values at room temperature for the materials used [22-29]*

Column Header Goes Here	Electrical Conductivity (S/m)	Thermal Conductivity (W/m.K)	Heat Capacity (J/kg.K)	Seebeck Coefficient (μV/K)
GST(Amorphous)	3	0.3	202	380
GST(Crystalline)	2770	0.7	202	47
Au	45.17 x 10^4	318	128	1.5
WTi	2.38 x 10^4	100	320	3.5
TiN	3.3 X 10^6	112	790	18

When an external voltage is applied to the PCM device, the first thing to be solved is Laplace equation,$\nabla.[\sigma\nabla F]$ =0 iteratively (with 5 ps time steps) for all mesh elements in electrical model. Here F is the spatial electrical potential distribution F(x,y,z), and σ is the electrical conductivity of the material. For crystalline and amorphous phases, electrical conductivity σ is 2770 S/m and 3 S/m, respectively [22]. However, it is important that in the simulation, σ has temperature and phase dependence and it changes during simulation running for each mesh element in every point and time. Therefore, there is an iterative solution in the simulation for all submodels.

In thermal model, with applied voltage, there is a current flow through the device causing joule heating ($Q = (JA)\ 2R\Delta t$) and heat diffusion equation should be solved iteratively to obtain temperature distribution T(x,y,z). Here, A, Δt, J, R are cross-sectional area, simulation time step, electrical current density and the resistance value of the material, respectively.

$$\nabla.J = -\nabla.\big(\sigma(\nabla V + S\nabla T)\big) = 0 \quad (1)$$

$$\mathrm{d}C_p\frac{dT}{dt} - \nabla.(\kappa\nabla T) = Q + Q_{th} \quad (2)$$

Where C is the heat capacity, j is the thermal conductivity. $Q_{th} = -TJ\nabla S$ accounts for the contribution of thermoelectric heat transport parameter, where S temperature dependence Seebeck coefficient and $\nabla S = dS\ dt\ \nabla T$ [15, 25]. Normally, heat diffusion equation includes Thomson effect and to avoid collapse of the modelling, Peltier effect was added into the simulation as a second heat source [18].

$$Q_{Thomson} = -TJ.\nabla\mathrm{S} \quad (3)$$

$$Q_{Peitier} = -J.\nabla\pi = -\mathrm{J}.\Delta(\mathrm{S}.\mathrm{T}) \quad (4)$$

At room temperature, for crystalline phase, thermal conductivity κ and Seebeck coefficient S value for GST material used in the simulation are 0.7 W/(Km) and 47 μV/K and, for amorphous phase, thermal conductivity κ and Seebeck coefficient S value are 0.3 W/(K m); 380 μV/K, respectively [15, 23, 25]. Beside the thermal conductivity κ and Seebeck coefficient, heat capacity for both phases is considers as a constant, 202 J/(kg K), for T<800 K. Also latent heat is taken into account in the calculations as a smooth Gaussian near the melting point (Tm=892 K).

Switching Dynamics

From the equations, it is easy to see that all parameters are temperature dependence. Therefore, phase change and final situation can be determined by temperature distribution. Switching dynamics includes phase change depending on the parameters and it follows forming crystalline nuclei and then its growth. However, there is an important point that due to heater electrode shape, there is heterogeneous phase configuration in the device. To obtain the probability rate for the crystallization process, phase change equation (5) should be solved. Forming nuclei and growth velocity of the nuclei, Vg,

$$dP\ dt = In\ (T)\ 1-P\ N + (T)\ 1-P\ a0 \quad (5)$$

Here (T) and $Vg(T)$ are nucleation and growth rates, P is the probability of crystallization, N the number of molecules per unit volume, and a0 is the atomic jump distance. (More detail in Cinar 2015)

Bruggeman effective medium approximation (EMA) is effective method to define physical properties of material, especially in crystal-amorphous phase mixture [30]. It can be easily determined electrical and thermal conductivity for each mesh element in the device.

$$(f, \sigma a, \sigma c) = 0.25 \{(2\sigma p - \sigma' p) + (2\sigma p - \sigma' p)\, 2 + (8\, \sigma a.\ )\, 1/2\ \} \qquad (6)$$

Here, f is the crystallization fraction. σa and σc are the electrical conductivity for amorphous and crystalline phases, respectively. With this formula, adding crystallization fraction into the simulation, the whole simulation is completed to observe the dynamics of phase change of the GST material during switching by connecting all submodel together.

Results and Discussion

First thing to do in the simulation is to find exact programming currents for set operation in case of with and without THT (Thomson and Peltier effects). Therefore from 0.5 V to 1 V external voltage was applied to the device for both cases and resistance versus voltage graphs were obtained. It is interesting that, from my previous studies, it is well known that square heater electrode possesses heterogonous temperature distribution due to the hot spots in the phase change material and this leads to inhomogeneous phase distribution which is actually mixture phase of crystalline and amorphous phase. However the obtained R-V graph is not expected for the without THT.

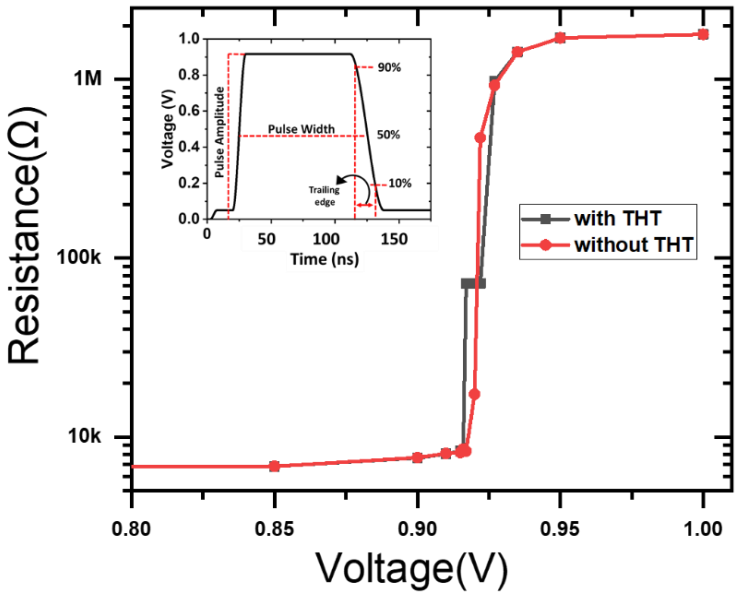

Figure 2. *Resistance versus voltage is plotted in the cases of with or without THT for square heater electrode. The applied voltage pulse amplitude is changed from 0.8 V to 1 V with 100 ns pulse width and 25ns trailing edge. Inset is the applied voltage pulse with amplitude of 0.92 V, 100 ns pulse width and 25 ns trailing edge.*

From the Figure 2, it is easily to see that for with THT, there is a stable middle resistance state occurring, but for without THT there is an abrupt switching from crystalline to amorphous state. Around 0.92 V for with THT, there is a middle resistance level with 72 kΩ. For crystalline state the resistance value is 6.8 kΩ. And the amorphous state resistance is 1.7 MΩ. There is roughly 1/10 ratio between crystalline and middle resistance level and roughly 1/24 ratio between middle and amorphous resistance level. To understand this results, temperature and phase change dynamics should be investigated.

An applied voltage pulse amplitude of 0.92 V, with 100 ns pulse width and 25 ns trailing edge was applied to the device for both cases of with and without THT and from the simulation, obtained temperature distribution inside the device for square heater electrode is illustrated in Figure 3 with a color map of local temperature. The behavior of temperature distribution for both cases are similar, however the maximum temperatures are different due to THT effect. Although the all parameters in both simulations are the same. From the Figure 3 c) and d) temperature distribution from the taken vertical slice at z=2 nm above the interface between TiN and GST has some hot spots originating from the shape effect of heater electrode caused by heterogeneous current flow because of sharp corner. In both cases, there are also hots spots with different maximum temperature. For with THT, the obtained maximum temperature is 953.92 K at t=70 ns (which is the time observing max temperature) and for without THT, maximum temperature is 942.65 K. The temperature difference very important, because the main parameter to determine the phase change of the GST is heating profile inside device. That means that with different temperature value, different phase change is obtained.

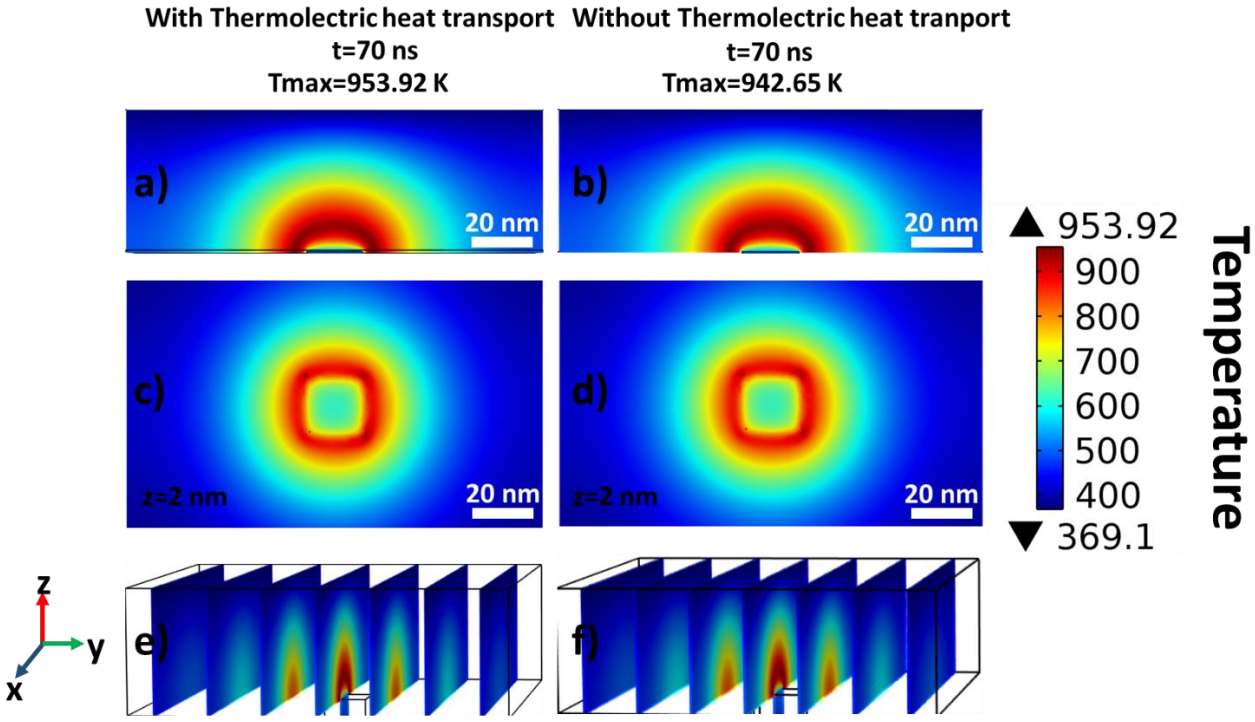

Figure 3. *A three dimensional illustration of temperature distribution at t=70 ns is plotted for different vertical and horizontal slices. a), b) and c) are for with THT, d), e) and f) are for without THT. a)–b) horizontal slice from the center of the device and c)–d) vertical slices at z=2 nm value, e)-f) horizontal slices for whole PCM layer. Illustration represent the temperature distribution inside PCM layer during an applied voltage pulse amplitude of 0.92 V, with 100 ns pulse width and 25 ns trailing edge.*

Initially, the phase change material is in crystalline phase and set operation is applied to the device to make switching from crystalline to amorphous phase. For a voltage pulse amplitude of 0.92 V, with 200 ns pulse width and 25 ns trailing edge, phase distribution is given in Figure 4. Images were taken from the central horizontal slice and color map of crystallization fraction is given for both cases in different time values. However, the interesting thing is that both cases start similar behavior, but after a certain time value, behaviors change because of THT effect. There is a sudden difference in without case at 147 ns. Normally, it looks like a mixture phase of amorphous and crystalline phase, and at 250 ns time value, Figure 4 i) and j) are the color phase distribution for both cases. As you can see from these images, but due to percolation there is a current flow passing though the device for without THT. Therefore, the resistance of the middle state of the with THT ($R \approx 72$ kΩ) is much more than without THT's resistance state ($R \approx 8.3$ kΩ) for a voltage pulse amplitude of 0.92 V, with 100 ns pulse width and 25 ns trailing edge. For this reason, to see the effect of THT effect, a point was taken into the device to observe the temperature change at this point. Figure 5 shows the temperature change in time for a given point with applying a voltage pulse amplitude of 0.92 V, with 100 ns pulse width and 25 ns trailing edge.

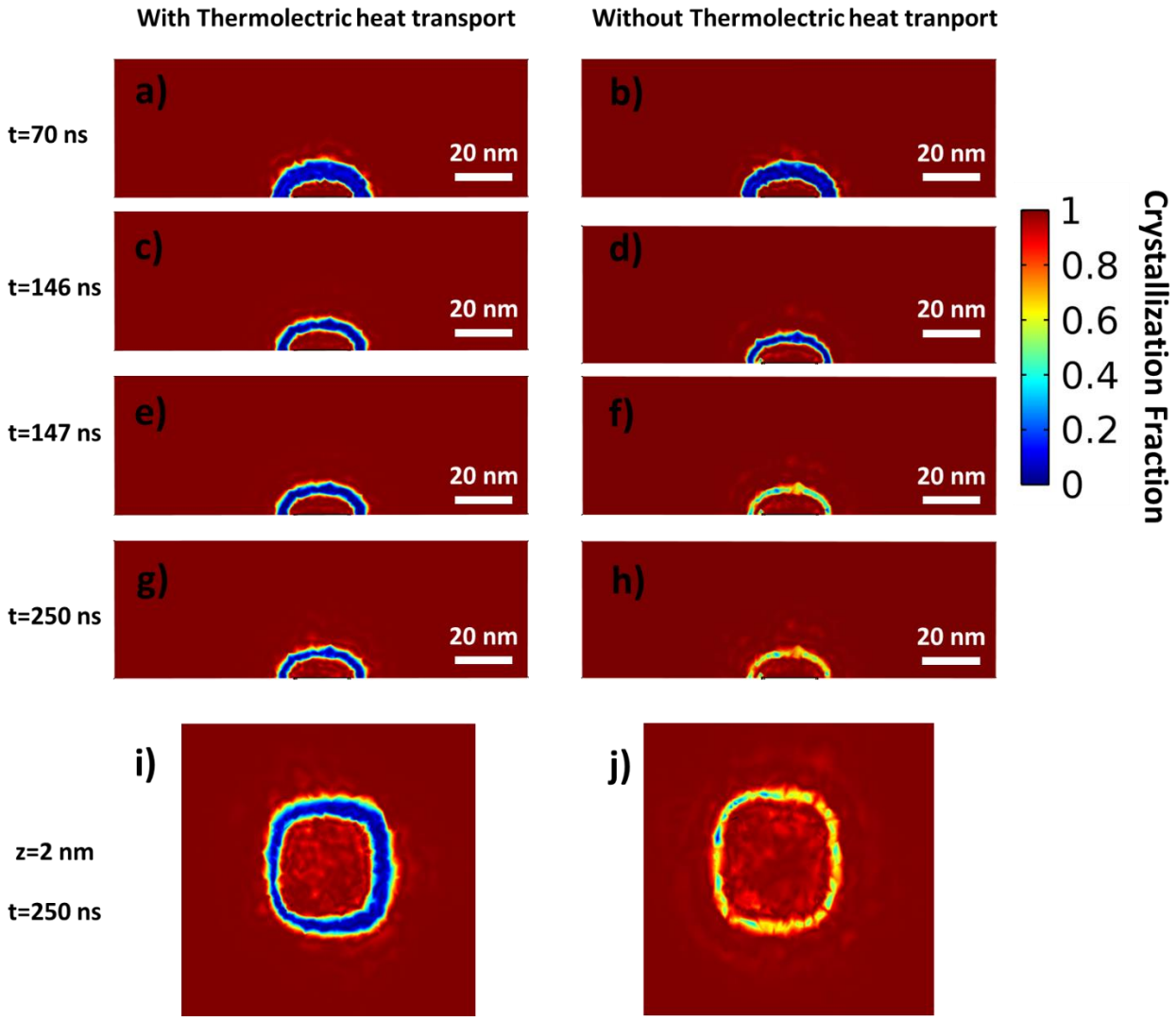

Figure 4. *Phase distribution of the device for an applied voltage pulse amplitude of 0.92 V, with 100 ns pulse width and 25 ns trailing edge is given by images taken from horizontal slices at different time. In different time range, the device phase changes were illustrated for both with and without THT cases. Crystallization fraction, f, is given with a color map. The color scale of crystallization fraction f=1 and f=0 corresponds red for crystalline and blue for amorphous phase respectively. Figure 4 a), c), e), g) and i) images are for without THT and Figure 4 b), d), f), h) and j) images are for without THT. Figure 4 i) and j) are vertical slices taking from z=2 nm above the interface between TiN and GST.*

In Figure 5 a), we can see the temperature change with time, but there is an unexpected behavior for with THT. With phase change, there is a temperature decrease and stabilizing phase. There is other increasing occurs. These two behaviors are well known due to switching, because changing phase affects the temperature change. However, at with THT, there is a sudden increase then temperature decrease similar to without THT. The reason behind this phenomena is the effect of THT. Because of hot spots around the phase change region, there is a current flow causing the temperature gradient and this effect can observe especially in short distance. Therefore for a given P point (z = 10 nm above the interface between TiN and GST layer), we observe this kind of an increase then decrease in cooling time. Figure 5 b) is the illustration of percolation path for current flow. Even though there is a phase change occurring at active region, if enough small path for current flow passing is enough for losing switching. Therefore to see the exact switching from crystalline to amorphous phase we need to obtain resistance change with voltage.

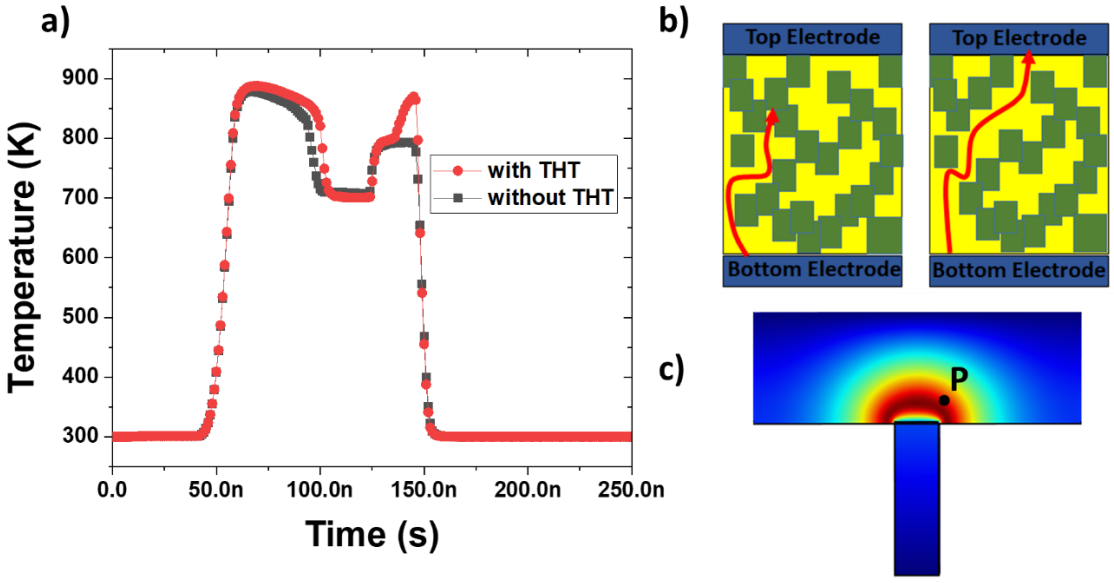

Figure 5. *Temperature change for a given P point the device. a) Temperature change b) percolation path c) Point P (z = 10 nm above the interface between TiN and GST layer) in the device.*

Conclusion

As a conclusion, to oversee the whole behavior of phase change switching of a PCM device, it is necessary to take into account for the THT (not only Thomson, but also Peltier effect) in the simulation, especially for heater electrode having heterogeneous heating profile. From the previous studies, square heater electrode causes inhomogeneous temperature distribution leading to middle resistance state between crystalline and amorphous state and with THT effect with Peltier effect the behavior of PCM device can be constructed correctly. Because, Peltier effect essentially should be considered around the interface and it has short distance effect, but for a small device and hot spots, Peltier effect must be included into the simulation due to closing the active region to interface. The whole THT effect has short range effect and it is not easy to see in bigger heater electrode device this effect. Modification of the simulation according to THT effect is essential in small square heater electrode PCM device. This helps us totally to visualize the nature switching dynamics of phase change material.

References

[1] Raoux, S., Wełnic, W., & Ielmini, D. (2010). Phase change materials and their application to nonvolatile memories. Chemical reviews, 110(1), 240-267

[2] Wong, H. S. P., Raoux, S., Kim, S., Liang, J., Reifenberg, J. P., Rajendran, B., & Goodson, K. E. (2010). Phase change memory. Proceedings of the IEEE, 98(12), 2201-2227.

[3] Wełnic, W., & Wuttig, M. (2008). Reversible switching in phase-change materials. Materials today, 11(6), 20-27.

[4] Yamada, N., Ohno, E., Akahira, N., Nishiuchi, K. I., Nagata, K. I., & Takao, M. (1987). High speed overwritable phase change optical disk material. Japanese Journal of Applied Physics, 26(S4), 61.

[5] Lee, B. C., Ipek, E., Mutlu, O., & Burger, D. (2009). Architecting phase change memory as a scalable dram alternative. In Proceedings of the 36th annual international symposium on Computer architecture (pp. 2-13).

[6] Pirovano, A., Lacaita, A. L., Benvenuti, A., Pellizzer, F., & Bez, R. (2004). Electronic switching in phase-change memories. IEEE Transactions on Electron Devices, 51(3), 452-459.

[7] Raoux, S., Burr, G. W., Breitwisch, M. J., Rettner, C. T., Chen, Y. C., Shelby, R. M., ... & Lam, C. H. (2008). Phase-change random access memory: A scalable technology. IBM Journal of Research and Development, 52(4.5), 465-479.

[8] Tominaga, J., Shima, T., Kuwahara, M., Fukaya, T., Kolobov, A., & Nakano, T. (2004). Ferroelectric catastrophe: beyond nanometre-scale optical resolution. Nanotechnology, 15(5), 411.

[9] Wuttig, M., & Yamada, N. (2007). Phase-change materials for rewriteable data storage. Nature materials, 6(11), 824-832.

[10] Liu, B., Zhang, T., Xia, J., Song, Z., Feng, S., & Chen, B. (2004). Nitrogen-implanted Ge2Sb2Te5 film used as multilevel storage media for phase change random access memory. Semiconductor science and technology, 19(6), L61.

[11] Gu, Y., Song, Z., Zhang, T., Liu, B., & Feng, S. (2010). Novel phase-change material GeSbSe for application of three-level phase-change random access memory. Solid-state electronics, 54(4), 443-446.

[12] Kao, K. F., Lee, C. M., Chen, M. J., Tsai, M. J., & Chin, T. S. (2009). Ga2Te3Sb5—A Candidate for Fast and Ultra long Retention Phase-Change Memory. Advanced materials, 21(17), 1695-1699.

[13] Rao, F., Song, Z., Zhong, M., Wu, L., Feng, G., Liu, B., & Chen, B. (2007). Multilevel data storage characteristics of phase change memory cell with double layer chalcogenide films (Ge2Sb2Te5 and Sb2Te3). Japanese journal of applied physics, 46(1L), L25.

[14] Hong, S. H., Lee, H., Choi, Y., & Lee, Y. K. (2011). Fabrication of multi-level switching phase change nano-pillar device using InSe/GeSbTe stacked structure. Current Applied Physics, 11(5), S16-S20.

[15] Cinar, I., Aslan, B., Gokce, A., Dincer, O., Karakas, V., Stipe, B., & Ozatay, O. (2015). Three dimensional finite element modeling and characterization of intermediate states in single active layer phase change memory devices. Journal of Applied Physics, 117(21).

[16] Price, P. J. (1956). Theory of transport effects in semiconductors: thermoelectricity. Physical Review, 104(5), 1223.

[17] Lee, J., Asheghi, M., & Goodson, K. E. (2012). Impact of thermoelectric phenomena on phase-change memory performance metrics and scaling. Nanotechnology, 23(20), 205201.

[18] Faraclas, A., Bakan, G., Dirisaglik, F., Williams, N. E., Gokirmak, A., & Silva, H. (2014). Modeling of thermoelectric effects in phase change memory cells. IEEE Transactions on Electron Devices, 61(2), 372-378.

[19] Suh, D. S., Kim, C., Kim, K. H., Kang, Y. S., Lee, T. Y., Khang, Y., & Ihm, J. (2010). Thermoelectric heating of Ge2Sb2Te5 in phase change memory devices. Applied Physics Letters, 96(12).

[20] Dirisaglik, F., Bakan, G., Faraclas, A., Gokirmak, A., & Silva, H. (2014). Numerical modeling of thermoelectric Thomson effect in phase change memory bridge structures. International Journal of High Speed Electronics and Systems, 23(01n02), 1450004.

[21] Bahl, J., Rajendran, B., & Muralidharan, B. (2015). Programming current reduction via enhanced asymmetry-induced thermoelectric effects in vertical nano pillar phase-change memory cells. IEEE Transactions on Electron Devices, 62(12), 4015-4021.

[22] Reifenberg, J. P., Kencke, D. L., & Goodson, K. E. (2008). The impact of thermal boundary resistance in phase-change memory devices. IEEE Electron Device Letters, 29(10), 1112-1114.

[23] Won, Y., Lee, J., Asheghi, M., Kenny, T. W., & Goodson, K. E. (2012). Phase and thickness dependent modulus of Ge2Sb2Te5 films down to 25 nm thickness. Applied physics letters, 100(16).

[24] Peng, C., Cheng, L., & Mansuripur, M. (1997). Experimental and theoretical investigations of laser-induced crystallization and amorphization in phase-change optical recording media. Journal of Applied Physics, 82(9), 4183-4191.

[25] Fiflis, P., Kirsch, L., Andruczyk, D., Curreli, D., & Ruzic, D. N. (2013). Seebeck coefficient measurements on Li, Sn, Ta, Mo, and W. Journal of nuclear materials, 438(1-3), 224-227.

[26] Kim, D. H., Merget, F., Först, M., & Kurz, H. (2007). Three-dimensional simulation model of switching dynamics in phase change random access memory cells. Journal of Applied Physics, 101(6).

[27] Lee, J., Kodama, T., Won, Y., Asheghi, M., & Goodson, K. E. (2012). Phase purity and the thermoelectric properties of Ge2Sb2Te5 films down to 25 nm thickness. Journal of Applied Physics, 112(1).

[28] Wang, L., Wen, J., Yang, C., & Xiong, B. (2018). Design of electrical probe memory with TiN capping layer. Journal of Materials Science, 53(22), 15549-15558.

[29] Yamamoto, T., Hatayama, S., Song, Y. H., & Sutou, Y. (2021). Influence of Thomson effect on amorphization in phase-change memory: dimensional analysis based on Buckingham's Π theorem for Ge2Sb2Te5. Materials Research Express, 8(11), 115902.

[30] Bruggeman, V. D. (1935). Berechnung verschiedener physikalischer Konstanten von heterogenen Substanzen. I. Dielektrizitätskonstanten und Leitfähigkeiten der Mischkörper aus isotropen Substanzen. Annalen der physik. 416, 7, 636-664.